

Characterization of excimer laser annealed polycrystalline $\text{Si}_{1-x}\text{Ge}_x$ alloy thin films by x-ray diffraction and spectroscopic ellipsometry

Guolin Yu^{a)}

Research Center for Micro-Structure Devices, Nagoya Institute of Technology, Gokiso-cho, Showa-ku, Nagoya 466, Japan

Kalaga Murali Krishna,^{b)} Chunlin Shao, and Masayoshi Umeno

Department of Electrical and Computer Engineering, Nagoya Institute of Technology, Gokiso-cho, Showa-ku, Nagoya 466, Japan

Tetsuo Soga^{c)}

Instrument and Analysis Center, Nagoya Institute of Technology, Gokiso-cho, Showa-ku, Nagoya 466, Japan

Junji Watanabe and Takashi Jimbo^{d)}

Research Center for Micro-Structure Devices, Nagoya Institute of Technology, Gokiso-cho, Showa-ku, Nagoya 466, Japan

(Received 28 March 1997; accepted for publication 29 September 1997)

Thin films of $\text{Si}_{1-x}\text{Ge}_x$ alloys of different compositions x have been deposited, on single-crystal Si (100) surface and glass substrates, by simple ion beam sputtering, at room temperature. Crystallization of these films has been done using excimer laser annealing. Structural and optical properties of as-deposited and annealed $\text{Si}_{1-x}\text{Ge}_x$ alloy films are characterized by x-ray diffraction (XRD), uv-visible spectrophotometry, spectroscopic ellipsometry (SE), and Auger electron spectroscopy (AES). The as-deposited films, both on Si and glass, have been found to be amorphous by XRD. Polycrystalline nature of laser-annealed samples has been evidenced by both x-ray and SE measurements. The results of x-ray, uv-visible, AES, and SE are compared and discussed. The poly- $\text{Si}_{1-x}\text{Ge}_x$ films were oriented predominantly to (111) and the grain sizes were determined from half-width of x-ray peaks. The compositions x of $\text{Si}_{1-x}\text{Ge}_x$ films have been evaluated from the SE dielectric function $\epsilon(\omega)$ data, using the second-derivative technique, and are found to be 0.23 and 0.36 for two different compositions. A detailed analysis of $\epsilon(\omega)$ with the effective-medium theory has demonstrated the volume fraction of crystalline $\text{Si}_{1-x}\text{Ge}_x$ increases with the increasing energy of laser irradiation. © 1998 American Institute of Physics. [S0021-8979(98)05301-8]

I. INTRODUCTION

Great interest has recently been devoted to $\text{Si}_{1-x}\text{Ge}_x/\text{Si}$ strained-layer heterostructures exhibiting attractive transport and optical properties. The $\text{Si}_{1-x}\text{Ge}_x$ alloy provides a continuously variable system with a wide range of optical band gaps. Polycrystalline silicon-germanium films are receiving considerable attention for applications such as high speed heterojunction bipolar transistors with the $\text{Si}_{1-x}\text{Ge}_x$ base formed by high-dose Ge implantation followed by solid-phase epitaxy.¹

Polycrystalline SiGe films can be an alternative to poly-Si in several technologies such as thin film transistors.^{2,3} Crystallization of amorphous silicon and amorphous silicon-germanium alloys, at low temperature, in short time, using excimer laser irradiation has been investigated by several authors.^{4,5} Furthermore, it is reported that pulsed laser-induced growth of poly- $\text{Si}_{1-x}\text{Ge}_x$ offers several advantages over alternative epitaxial processes.⁶ The heterojunction and quantum well structures of this alloy system do also

have potential for optoelectronic devices such as modulators, switches, and detectors.^{7,8} Recently, Nelson *et al.*⁹ have studied the Ohmic contacts to n -type silicon-germanium alloys and suggested that an alloy of silver and antimony will be a more reliable metal contact for Si/ $\text{Si}_{1-x}\text{Ge}_x$ n -type heterostructures over the commonly used Au/Sb alloyed contacts.

Also, spectroscopic ellipsometry (SE) is known as a nondestructive and nonperturbing technique to characterize thickness, structure, composition, and various optical properties of thin films. Using SE, Humlicek *et al.*¹⁰ have produced a series of pseudodielectric ($\epsilon = \epsilon_1 + i\epsilon_2$) functions for a number of bulk $\text{Si}_{1-x}\text{Ge}_x$ alloys of composition $x = 0.22, 0.39, 0.51, 0.64, 0.75, 0.83,$ and $0.91,$ and determined the critical point energies by fitting the numerically differentiated dielectric functions. Nguyen *et al.*¹¹ have used SE to investigate the properties of the interface between Ge-implanted Si and its thermal oxide and interpreted the data in terms of a $\text{Si}_{1-x}\text{Ge}_x$ alloy using the measured spectrum of Humlicek *et al.* SE of strained and relaxed $\text{Si}_{1-x}\text{Ge}_x$ epitaxial layers of arbitrary compositions were also studied by others.^{12,13} However, little work has been done on optical and structural characterization of poly- $\text{Si}_{1-x}\text{Ge}_x$ alloy thin films for their potential application in optoelectronic devices such as solar cells.

^{a)}Electronic mail: yu@gamella.elcom.nitech.ac.jp

^{b)}Present address: Research Center for Micro-Structure Devices.

^{c)}Present address: Department of Environmental Technology and Urban Planning.

^{d)}Present address: Department of Environmental Technology and Urban Planning.

Here, we propose ion beam sputtering as a simple and convenient method for the deposition of arbitrary compositions of $\text{Si}_{1-x}\text{Ge}_x$ alloy thin films and excimer laser irradiation for the crystallization of as-deposited films for the future application of Si/SiGe based superlattice structures as solar cell devices. In this article, we report the crystal structure, composition, and optical properties of both, as-deposited and laser-annealed, films characterized by x-ray diffraction (XRD), uv-visible spectroscopy, Auger electron spectroscopy (AES), and SE. We determined the composition of crystallized $\text{Si}_{1-x}\text{Ge}_x$ thin films using the analysis of the experimental $\epsilon(\omega)$ with the second-derivative technique. The effects of surface treatment of our films, polished using Syton-saturated lens paper, on optical properties, are studied in terms of critical point (CP) energies, strongly depends on the composition of the alloy system, and may be shifted due to the oxidation/roughening.¹³ We further discuss the volume fraction of crystalline $\text{Si}_{1-x}\text{Ge}_x$ using the interpolation procedure developed by Snyder *et al.*¹⁴ and the effective-medium theory (EMT). The dielectric functions of $\text{Si}_{1-x}\text{Ge}_x$ alloys are taken from the literature.¹⁰

II. EXPERIMENT

A germanium target, partly covered with silicon wafers, has been used for the deposition of $\text{Si}_{1-x}\text{Ge}_x$ alloy thin films, of different compositions (x), by Ar^+ ion beam sputtering. Single-crystal Si (100), 2° off towards [011], and glass are used as substrates. The arbitrary composition can simply be controlled by varying the area of Si wafers. The deposition has been carried at a base pressure of 2×10^{-6} Torr, and at room temperature, using the beam voltage of 1 kV, beam current of 20 mA, and power of 20 W. These films have been analyzed by various analytical techniques and the results are discussed in the following sections.

The resulting films are smooth with excellent adhesion to the substrate. Crystallization was carried out at room temperature and in air using a XeCl excimer laser ($\lambda = 308$ nm) which provides an area of $5 \text{ mm} \times 5 \text{ mm}$ and pulses of 20 ns (full width at half-maximum) duration. Samples were annealed by the irradiation of one laser pulse, and the energy of laser irradiation was varied and different laser pulse energies of 92–212 mJ/cm^2 were used. Details concerning the laser irradiation conditions for various samples studied are listed in Table I.

The structural characterization and grain size determination of the films are performed using an x-ray diffractometer with $\text{CuK}\alpha$ radiation. All the patterns are recorded at an angular speed as low as $0.2^\circ/\text{min}$ by steps of 0.02° and with a voltage of 40 kV and current of 35 mA in the standard $\theta-2\theta$ geometry. The crystallographic preferred orientation of polycrystalline films is measured by comparing the intensity of the different diffraction peaks with a randomly oriented polycrystalline film, and the integral linewidth and Bragg angle are determined by fitting directly the diffraction profile using the convolution equation between the pure profile and the Deby–Scherrer instrumental profile, and are discussed in detail in the following x-ray section. The optical transmission in the wavelength range (between 400–1600 nm) was measured using an uv-visible spectro-

TABLE I. Experimental details of ion beam sputtered poly- $\text{Si}_{1-x}\text{Ge}_x$ alloy thin films.

Sample no.	Substrate	Composition (x)	Energy of laser irradiation (mJ/cm^2)
1	Glass	0.23 ± 0.01	212
2	Glass	0.23 ± 0.01	164
3	Si	0.23 ± 0.01	212
4	Si	0.23 ± 0.01	164
5	Glass	0.36 ± 0.01	212
6	Glass	0.36 ± 0.01	164
7	Si	0.36 ± 0.01	212
8	Si	0.36 ± 0.01	164

photometer. The composition and formation of $\text{Si}_{1-x}\text{Ge}_x$ alloys have been realized from surface and depth profile analyses using AES.

Since the CP energy strongly depends on the composition of $\text{Si}_{1-x}\text{Ge}_x$ alloys and also may be shifted due to the oxidation/roughening,¹³ it is necessary to treat the surface before SE measurements in order to estimate the composition of poly- $\text{Si}_{1-x}\text{Ge}_x$. Therefore, we have polished our samples with Syton-saturated lens paper, followed by a rinse with water. This process was repeated until the largest value of ϵ_2 at E_2 (about 4.3 eV) was obtained. Optical data were recorded with a polarizer-sample-rotating-analyzer spectroellipsometer, at room temperature. Variable angle-of-incidence spectroscopic ellipsometry has been measured, for samples sputtered on both the glass and Si substrates, in the wavelength range of 260–830 nm with a step of 5 nm, at an angle of incidence 60° . During the measurement the surface-treated samples were maintained in a drying N_2 flow to eliminate various surface contamination effects. All the SE plots presented in this article are for samples deposited on glass substrate. However, the data obtained from SE measurement of samples deposited on Si substrate are tabulated and discussed in the respective following sections.

III. RESULTS AND DISCUSSION

A. X-ray diffraction

Figure 1 shows the x-ray diffraction patterns on samples of as-deposited [pattern (a)] and laser-annealed [patterns (b), (c), (d), and (e), respectively, for samples 1, 3, 5, and 7] structures of two different $\text{Si}_{1-x}\text{Ge}_x$ compositions, $\{x=0.23$ [(b) and (c)] and $x=0.36$ [(d) and (e)], these compositions are derived from SE measurements and are discussed in the following section}, deposited on Si [(a), (c), and (e)] and glass [(b) and (d)] substrates by ion beam sputtering. In the as-deposited case, with both the substrates, we observe the amorphous nature of the thin film with two halos [Fig. 1(a), on Si substrate]. The first, centered at $2\theta=28^\circ$ close to the position of the (111) crystalline diffraction peak corresponds to the existence of a short-range diamond cubic structure. And the other, located at covering $2\theta=45^\circ-55^\circ$ may be due to the (220) and the (311) crystalline peaks. For laser, an-

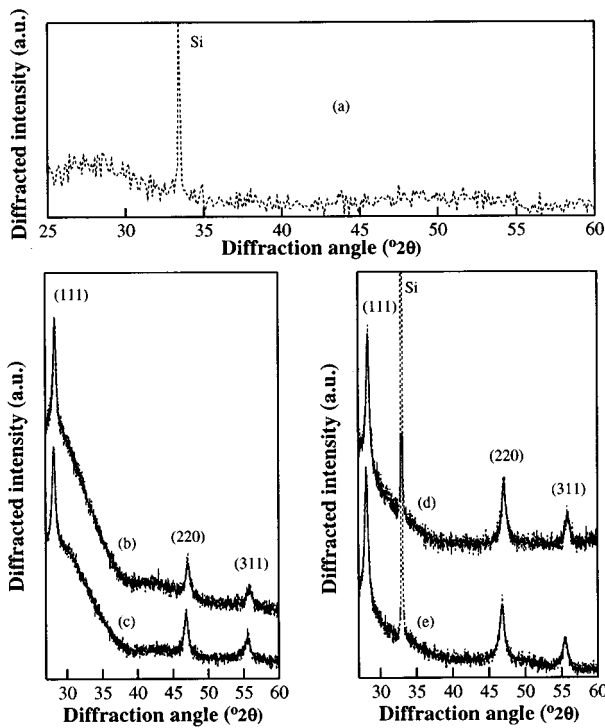


FIG. 1. X-ray diffraction patterns of ion beam sputtered $\text{Si}_{1-x}\text{Ge}_x$ alloy thin films of as-deposited [(a)] and laser irradiated [(b)–(e)] samples of two different compositions, $x=0.23$ [(b) and (c)] and $x=0.36$ [(d) and (e)], deposited on Si [(a), (c), and (e)] and glass [(b) and (d)] substrates. (a) As-deposited, (b) sample 1, (c) sample 3, (d) sample 5, and (e) sample 7. Experimental curves are very well fitted (solid line) with the function mentioned as Eq. (2).

nealed samples, the three peaks corresponding to (111), (220), and (311) indicate the polycrystalline nature of the films upon laser irradiation.

To determine the grain size of the samples it is necessary to correct lines for the experimental aberrations. In order to obtain the Deby–Scherrer instrumental profile $g(\epsilon)$, we measured larger-grain-size polycrystalline silicon powder,¹⁵ and the experimental profile is very well fitted with the function.¹⁶

$$f(x) = C/[1 + (x/k)^2]^2. \quad (1)$$

In the above expression, C and k are adjustable constants and x is the abscissa measured from the profile maximum.

An experimental profile $h(\epsilon)$, that is directly observable, is the convolute between a weight function $g(\epsilon)$ and a pure diffraction profile $f(\epsilon)$,¹⁷

$$h(\epsilon) = \int_{-\infty}^{\infty} g(\zeta)f(\epsilon - \zeta)d\zeta. \quad (2)$$

A pure diffraction profile free of instrumental contributions $f(\epsilon)$ in Eq. (2), is also assumed as Eq. (1). Experimental profiles of the $\text{Si}_{1-x}\text{Ge}_x$ alloys of two different compositions (Fig. 1) are well fitted using Eq. (2) as shown in Fig. 1 by solid lines. And, the integral linewidth has been determined for these line profiles in order to evaluate the grain size l , using the classical Scherrer equation,

$$l = k_s \lambda / \Delta \cos \theta, \quad (3)$$

where θ is the Bragg angle, λ the wavelength of the radiation used, k_s a constant¹⁵ closed to 1.05, and Δ is the integral linewidth. In order to determine the crystallographic preferred orientation of growth, we calculated the normalized intensity ratio of each sample i α_i and β_i defined by

$$\alpha_i = I_{i(220)} / I_{p(220)},$$

$$\beta_i = I'_{i(311)} / I'_{p(311)},$$

where $I_i = C_{i(220)} / C_{i(111)}$ and $I'_i = C_{i(311)} / C_{i(111)}$ are the intensity ratios of the pure diffraction profiles determined by fitting, and I_p and I'_p are the fractions measured from the intensities of the Bragg peaks for the standard randomly oriented silicon powder infinitely thick, which takes into account the absorption coefficient of the film for the radiation used.¹⁵ The results are listed in Table II. These results indicate that the (111) orientation is dominant in the samples deposited on both glass and Si substrates, together with the orientation dominance of (311) peak in the case of samples deposited on Si substrate: this is associated with the difference of free surface energy between the Si and glass substrates. Under the excimer laser irradiation, it is reported that the recrystallization starts from the surface of amorphous Si deposited over the glass substrate and the (111) orientation was dominant.¹⁸ Therefore, the free surface energy of a film also plays an important role, the same as in the case of UHV-annealed amorphous Si on quartz.¹⁹ On the other

TABLE II. X-ray diffraction results of poly- $\text{Si}_{1-x}\text{Ge}_x$ alloy thin films.

Sample no.	$\langle 111 \rangle$			$\langle 220 \rangle$			$\langle 311 \rangle$			α	β
	2θ (°)	k	Grain size (nm)	2θ (°)	k	Grain size (nm)	2θ (°)	k	Grain size (nm)		
1	28.262 ± 0.005	0.342 \pm 0.01	86.2	47.047 ± 0.01	0.496 \pm 0.03	36.4	55.769 ± 0.02	0.688 \pm 0.06	22.4	0.61	0.64
3	28.274 ± 0.005	0.333 \pm 0.02	88.4	47.025 ± 0.01	0.323 \pm 0.04	55.9	55.785 ± 0.02	0.521 \pm 0.04	29.5	0.68	0.94
5	28.097 ± 0.005	0.383 \pm 0.01	77.4	46.768 ± 0.008	0.511 \pm 0.02	34.8	55.460 ± 0.02	0.654 \pm 0.04	23.7	0.76	0.80
7	28.090 ± 0.04	0.377 \pm 0.01	78.6	46.754 ± 0.01	0.433 \pm 0.04	41.1	55.456 ± 0.01	0.630 \pm 0.03	24.6	0.66	0.93

hand, the Si substrate could act as a seed for crystal growth for the excimer laser annealing process.²⁰ Since the Si (100) 2° off towards [011] was used as a substrate in our experiments, the surface of Si substrates are composed of deformed steps of molecular dimensions, thus the simultaneous dominance of {311} planes is not surprising.¹⁵ Also, from Table II, it is clear that the grain size decreases with increasing Ge mole fraction irrespective of the substrate used (either Si or glass) and this may be explained as follows. Y. Morita *et al.*²¹ had reported that the grain size increases with the increasing energy of laser irradiation for amorphous Si on glass. Furthermore, our SE measurements show that the absorption spectrum shifts towards longer wavelengths and the absorption coefficient decreases with increasing Ge mole fraction for amorphous Si_{1-x}Ge_x films at the wavelength of excimer laser (308 nm). Combining the two observations of Morita *et al.* and our SE measurements, we can say that under the same energy of laser irradiation, different amounts of laser energy were absorbed by the deposited films due to the variation in the composition, which alters the degree of annealing and hence the change in the degree of crystallinity.

The lattice parameters of Si_{1-x}Ge_x alloys of the two different compositions are found to be 5.465 and 5.496 Å, respectively. It is observed that the lattice parameter increases with increasing Ge concentration. The difference in composition between the samples of two different Ge concentrations can be estimated from the plot of lattice constant versus Ge mole fraction, assuming a linear relation between the lattice constants of Si (5.430 95 Å) and Ge (5.64613 Å).²² It is found to be 0.144, which is in agreement with the value (0.13) obtained by SE. However, we cannot rule out the effect of strain present in our samples. An analysis of strain has been discussed together with the ellipsometric results in the following section.

B. Spectroscopic ellipsometry

The pseudodielectric function is given by

$$\langle \epsilon \rangle = \langle \epsilon_1 \rangle + i \langle \epsilon_2 \rangle = \sin^2 \phi \left\{ 1 + \left[\frac{(1-\rho)}{(1+\rho)} \right]^2 \tan^2 \phi \right\}, \quad (4)$$

where ϕ is the angle of incidence. Note that ϵ is a quantity derived from the SE data using the two-phase (ambient/substrate) model, and therefore corresponds to samples where there is no overlayer. The pseudodielectric function spectra (ϵ_1 and ϵ_2) of as-deposited, laser-irradiated, and Syton-polished Si_{1-x}Ge_x alloys of two different compositions $x=0.23$ and 0.36 (samples 1 and 5) are shown in Figs. 2 and 3, respectively. In the same Figs. 2 and 3, the dielectric function of Si_{1-x}Ge_x alloys of the two compositions ($x=0.23$ and 0.36) obtained from the interpolation procedure¹⁰ and that of poly-Si (Ref. 23) were also plotted for comparison. It is clear from these figures that the as-deposited films are amorphous and convert to poly-Si_{1-x}Ge_x after excimer laser irradiation. The analysis of pseudodielectric function spectra of laser-irradiated samples, using a four-phase (ambient/SiO₂/rough layer/poly-Si_{1-x}Ge_x) model, has demonstrated that the samples consist of about 6.8 nm overlayer on the surface. Further, the Syton-polished samples have larger values of ϵ_2 at E_2 (about 4.3 eV) compared with

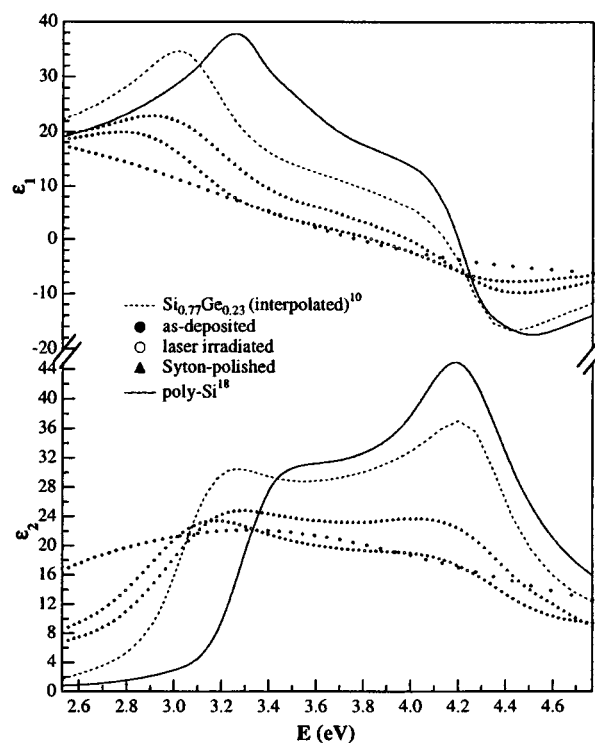


FIG. 2. The pseudodielectric function spectra ($\epsilon = \epsilon_1 + i\epsilon_2$) of as-deposited, laser-irradiated (sample 1), and Syton-polished surface of sample 1. The dielectric function spectra of poly-Si and the interpolated spectrum of Si_{0.77}Ge_{0.23} are also shown for comparison.

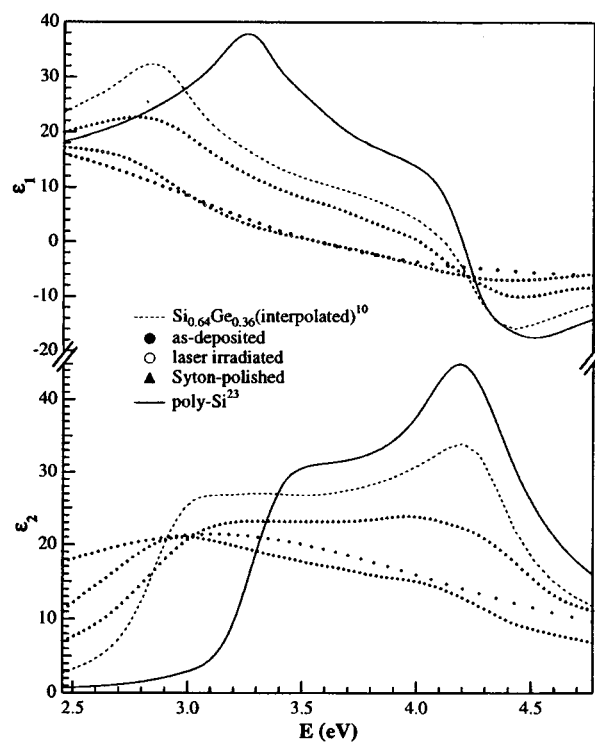


FIG. 3. The pseudodielectric function spectra ($\epsilon = \epsilon_1 + i\epsilon_2$) of as-deposited, laser-irradiated (sample 5), and Syton-polished surface of sample 5. The dielectric function spectra of poly-Si and the interpolated spectrum of Si_{0.64}Ge_{0.36} are also shown for comparison.

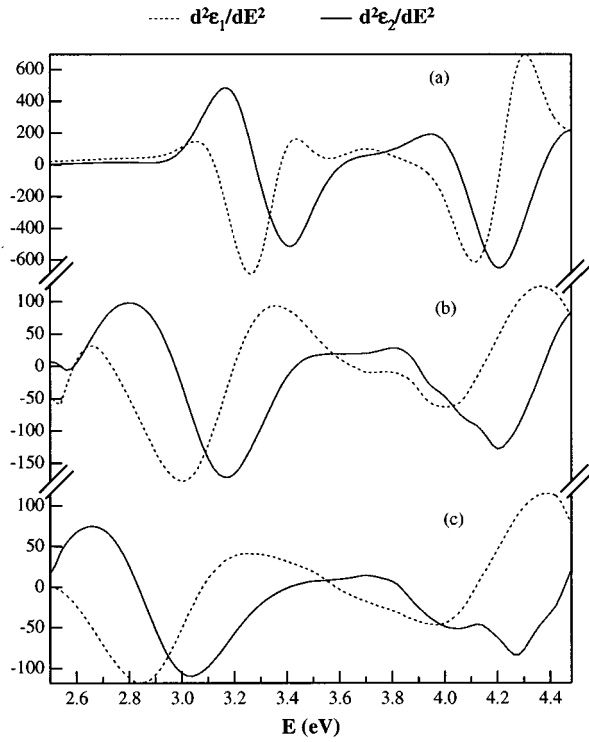


FIG. 4. The numerically differentiated second-derivative spectra of ($\epsilon = \epsilon_1 + i\epsilon_2$) for (a) poly-Si (Ref. 23), and our Syton-polished samples (b) sample 1 and (c) sample 5.

that of the laser-irradiated (unpolished) surface (Figs. 2 and 3). Therefore, these samples are assumed to have close to ideal surface quality, and further analysis was done only on Syton-polished samples by both SE and transmission measurements.

The structure in the vicinity of the so-called points CPs that appear in $\epsilon(\omega)$ can be analyzed in terms of standard analytic line shapes. The two-dimensional CP and the $\epsilon(\omega)$ can be expressed as

$$\epsilon(\omega) \approx A \ln(E_g - \omega + i\Gamma) e^{i\phi}, \quad (5)$$

where A describes the amplitude, E_g the threshold energy of the CP, Γ its broadening, and ϕ the phase angle.

The experimental second derivative (obtained by numerical differentiation of the original spectra) can enhance the structure in the spectra and the line-shape analysis of the CP can be performed using least squares in order to determine the parameters E_g , A , Γ , and ϕ . In Fig. 4, the second-derivative spectrum of our laser-irradiated poly-Si_{1-x}Ge_x alloys for two different compositions, $x = 0.23$ (b) and $x = 0.36$ (c) are shown and compared with that of poly-Si (a).²³ The structures from our poly-Si_{1-x}Ge_x, attributed to E_1 ($L_3^y \rightarrow L_3^c$) and E_2 ($X_4^y \rightarrow X_1^c$) transitions, can be clearly seen from Fig. 4, and it is evident that the peak of E_1 shifts toward lower energy compared to the poly-Si.

The results of the second-derivative analysis of the E_1 structure assuming one CP are given in Table III. It is reported that the Si_{1-x}Ge_x films on Si substrate are under compressive stress,¹³ and the thicker (above 40 nm) poly-Si films on SiO₂ exhibit internal tensile stress.²⁴ However, it is clear from Table III that the values of E_1 have no obvious differ-

TABLE III. The E_1 interband transition parameters (amplitude A , threshold energy E_g , broadening Γ , and phase angle ϕ) obtained by fitting the second derivative of the dielectric function spectra of poly-Si_{1-x}Ge_x alloy thin films.

Sample no.	A	E_g (eV)	Γ (meV)	ϕ (°)
1	54.8	3.086	147	-0.76
2	49.4	3.076	157	-1.64
3	52.8	3.088	163	-0.303
4	48.1	3.078	169	-16.08
5	47.1	2.895	175	-20.39
6	43.7	2.877	190	-8.96
7	40.8	2.905	169	-10.97
8	40.8	2.903	185	-13.97

ence, irrespective of the substrate used (either Si or glass), for a particular composition. Hence, we estimate all our films are relaxed from the strain in the near surface because the penetration depth of the light beam is about 10 nm at around E_1 peak wavelength. Therefore, the shift in the E_1 peak energies between the poly-Si_{1-x}Ge_x [Figs. 4(b) and 4(c)] and poly-Si [Fig. 4(a)] is mainly attributed to the Ge mole fraction. Furthermore, the shift between the two different compositions [Figs. 4(b) and 4(c)] indicates the difference in the concentration of Ge in poly-Si_{1-x}Ge_x alloys. The mole fraction of Ge has been evaluated according to the relation between the composition (x) and E_1 developed by Humlicek *et al.* and found to be about 0.23 ± 0.01 and 0.36 ± 0.01 for two different compositions. These results are in agreement with x-ray and AES measurements which reveal the formation of Si_{1-x}Ge_x alloys of two different compositions. Using these compositions, once again according to the linear relationship mentioned in the x-ray section, the lattice constants of Si_{1-x}Ge_x alloys of two different compositions $x = 0.23$ and 0.36 are found to be 5.480 and 5.508 Å, respectively. These values are slightly larger than those obtained by x-ray analyses (5.465 and 5.496 Å), maybe due to the influence of microstrain which is neglected for SE measurements as mentioned above. However, the slight difference in lattice parameters obtained from the two different techniques, for the same composition, may be related to the presence of strain. Hence, it is clear from these results that the shift in diffraction peaks for the two different compositions is not only due to the difference in Ge concentration but also due to the compressive strain as is evidenced from the difference in lattice parameters obtained from XRD and SE measurements. The magnitude of the strain was estimated to be -0.003 , which is almost more than half that of single-crystalline Si_{0.78}Ge_{0.22} grown on Si substrate.¹³ However, this strain does not change the results of grain size as it is a uniform compressive strain.²⁵ The values of broadening (Γ) have been interpreted in terms of the mean grain size of the poly-Si_{1-x}Ge_x alloys and similar conclusions have been derived earlier in case of poly-Si thin films.²⁴ However, no matter what substrates are used, in a particular composition, the broadening decreases (i.e., grain size increases) with increasing energy of laser irradiation.

In order to obtain quantitative information through the analysis of the SE measurements (Δ, Ψ), we have calculated

TABLE IV. The best fit parameters determined by SE measurements. The 90% confidence limits are given with (\pm). Also, the optical gap E_{04} , the energy at which the absorption coefficient α is 10^4 cm^{-1} , measured by uv-visible spectroscopy is presented.

Sample no.	Composition			Thickness (nm)	δ	E_{04} (eV)	
	$c\text{-Si}_{1-x}\text{Ge}_x$	$a\text{-SiGe}$	Void				
1		0.692 ± 0.02	0.222 ± 0.02	0.086	257.0 ± 2.1	0.045	1.28
2	$x=0.23$ ± 0.01	0.578 ± 0.02	0.335 ± 0.02	0.087	260.8 ± 2.6	0.048	1.19
3		0.602 ± 0.03	0.332 ± 0.03	0.066	263.1 ± 5.7	0.035	-
4		0.494 ± 0.02	0.431 ± 0.03	0.075	253.4 ± 5.0	0.027	-
5		0.728 ± 0.02	0.209 ± 0.02	0.063	271.3 ± 2.4	0.038	1.15
6	$x=0.36$ ± 0.01	0.588 ± 0.02	0.316 ± 0.02	0.096	283.2 ± 3.0	0.039	1.05
7		0.591 ± 0.03	0.349 ± 0.04	0.060	275.9 ± 8.8	0.045	-
8		0.488 ± 0.03	0.461 ± 0.03	0.051	285.4 ± 9.0	0.039	-

the dielectric function of poly- $\text{Si}_{1-x}\text{Ge}_x$ of composition $x=0.23$ and $x=0.36$ according to the interpolation procedure developed by Snyder *et al.* We analyzed SE data of the Syton-polished poly- $\text{Si}_{1-x}\text{Ge}_x$ surface using a three-phase (ambient/poly- $\text{Si}_{1-x}\text{Ge}_x/\text{Si}$ or glass substrate) model. The poly- $\text{Si}_{1-x}\text{Ge}_x$ is assumed as a composite material consisting of crystalline $\text{Si}_{1-x}\text{Ge}_x$, amorphous $\text{Si}_{1-x}\text{Ge}_x$ and void. The dielectric response of these films was represented by the Bruggeman effective-medium theory EMT. The mathematical formula can be expressed as

$$\sum_i^n f_i \frac{\epsilon_i - \epsilon}{\epsilon_i + 2\epsilon} = 0, \quad (6)$$

where ϵ_i and f_i ($\sum f_i = 1$) are the dielectric function and volume fraction, respectively, of the i th component. The unknown parameters can be numerically determined by minimizing the following mean squares deviation with a regression program (unbiased):²⁴

$$\delta^2 = \frac{1}{(N-P-1)} \left(\sum_{i=1}^N |\rho_i^{\text{exp } t} - \rho_i^{\text{calc}}|^2 \right), \quad (7)$$

where N is the number of data points and P is the number of unknown model parameters. All the parameters derived from this analysis are summarized in Table IV. It is to be noted that our poly- $\text{Si}_{1-x}\text{Ge}_x$ alloy thin film has the density deficit because the void fraction is positive. However, this deficit is larger in films deposited on glass over that of Si. Moreover, it is obvious from these results that the density and the volume fraction of crystalline $\text{Si}_{1-x}\text{Ge}_x$ increases with increasing energy of laser irradiation. Also, it is to be noted that the volume fraction of crystalline $\text{Si}_{1-x}\text{Ge}_x$ of films deposited on glass substrate is slightly larger than that of films on Si substrate, irrespective of the composition x . This may be be-

cause the time of recrystallization on Si substrate is shorter than that on glass substrate because, the thermal conductivity of Si is larger than glass.

C. Ultraviolet-visible absorption spectroscopy

Figure 5 shows the spectrum of absorption coefficient versus photon energy for Syton-polished samples 1 and 5 from the uv-visible transmission measurements. Since the Tauc's gap is not valid for microcrystalline or biphasic materials,²⁶ the optical gap of our $\text{Si}_{1-x}\text{Ge}_x$ alloys of two

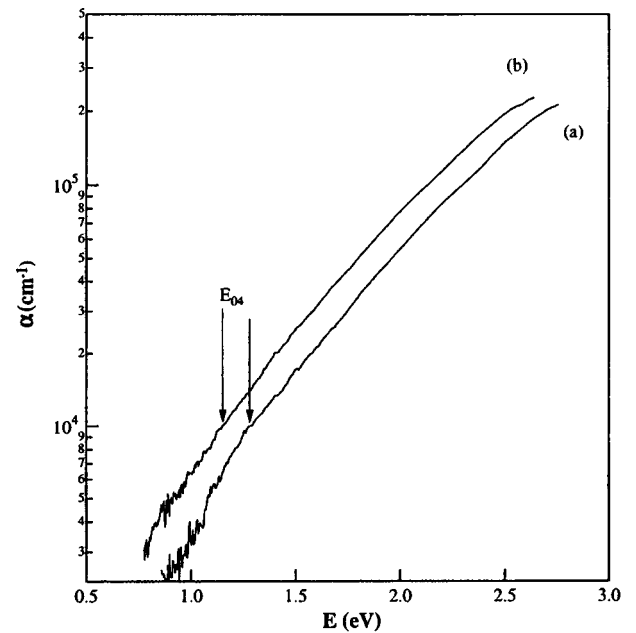


FIG. 5. Plots of absorption coefficient α vs photon energy E , for Syton-polished surface of samples 1 and 5 [(a) and (b), respectively], in order to obtain the optical gap of the films in terms of E_{04} (defined as the energy at which α is equal to 10^4 cm^{-1}).

different compositions are evaluated in terms of E_{04} , the energy at which the absorption coefficient (α) is 10^4 cm^{-1} .^{27,28} These values are listed in Table IV. It is clear from Tables I and IV that the E_{04} decreases with increasing Ge mole fraction and decreasing the energy of laser irradiation. These results further support the conclusions derived from the x-ray and SE, that the degree of crystallinity depends on the energy of laser irradiation and amount of Ge concentration, the two key factors which determine the value of E_{04} .

IV. CONCLUSIONS

Amorphous thin films of $\text{Si}_{1-x}\text{Ge}_x$ alloys have been deposited on glass and single-crystal Si substrates by ion beam sputtering, and the composition (x) is controlled by varying the area of silicon wafers placed on the germanium target. Upon XeCl excimer laser annealing, these films reveal polycrystalline nature by both x-ray and SE measurements. The composition (x) of $\text{Si}_{1-x}\text{Ge}_x$ films, evaluated from the SE dielectric function $\epsilon(\omega)$ data using the second-derivative technique, is in agreement with those obtained from x-ray and AES measurements within their experimental limitations.

It has also been observed that the (111) orientation is predominant in all of poly- $\text{Si}_{1-x}\text{Ge}_x$ films on both the substrates. This dominance of (111) orientation is attributed to the free surface energy of films which plays a major role in the crystallization process. Furthermore, the detailed analysis of x-ray diffraction data and SE measurements show that the average microcrystallite size decreases with increasing Ge mole fraction, and the volume fraction of crystalline $\text{Si}_{1-x}\text{Ge}_x$ increases with increasing laser-irradiation energy. These phenomena have been attributed to different degrees of annealing and hence the changing in the degree of crystallinity.

Finally, the optical gap of these films has been obtained in terms of E_{04} (defined as the energy at which α is equal to 10^4 cm^{-1}) from the absorption coefficient spectra and the value is found to be in the range of 1.05–1.28 eV for two Ge concentrations. These results further support the conclusion that the $\text{Si}_{1-x}\text{Ge}_x$ alloy provides continuously and widely variable optical band gap. These results promise future scope of this material in solar cell application and the work is in progress in our group.

ACKNOWLEDGMENTS

This work is supported by Fujimi Inc. and the Ministry of Education, Government of Japan.

- ¹S. Lombardo, A. Pinto, V. Raineri, P. Ward, G. La Rosa, G. Privitera, and S. U. Campisano, *IEEE Electron Device Lett.* **17**, 485 (1996).
- ²A. Slaoui, C. Deng, S. Talwar, J. K. Kramer, and T. W. Sigmon, *Appl. Phys. A: Solids Surf.* **59**, 203 (1994).
- ³I. Manna, L.-T. Jung, and S. Banerjee, *IEEE Proceedings of the 53rd Annual Device Res. Conference Digest*, 1995, p. 156.
- ⁴E. A. Al-Nuaimy and J. M. Marshall, *Appl. Phys. Lett.* **69**, 3857 (1996).
- ⁵A. Slaoui, C. Deng, S. Talwar, J. K. Kramer, B. Prevot, and T. W. Sigmon, *Mater. Res. Soc. Symp. Proc.* **321**, 689 (1994).
- ⁶A. Slaoui, C. Deng, S. Talwar, J. K. Kramer, T. W. Sigmon, J. P. Stoquert, and B. Prevot, *Appl. Surf. Sci.* **86**, 346 (1995).
- ⁷X. Zhang, Z. Chen, D. Cui, G. Yang, and R. Wang, *Appl. Phys. Lett.* **69**, 3164 (1996).
- ⁸D. Labrie, G. C. Aers, H. Lafontaine, R. L. Williams, S. Charbonneau, R. D. Goldberg, and I. V. Mitchell, *Appl. Phys. Lett.* **69**, 3866 (1996).
- ⁹S. F. Nelson and T. N. Jackson, *Appl. Phys. Lett.* **69**, 3563 (1996).
- ¹⁰J. Humlicek, M. Garriga, M. I. Alonso, and M. Cardona, *J. Appl. Phys.* **65**, 2827 (1989).
- ¹¹N. V. Nguyen, K. Vedam, and J. Narayan, *J. Appl. Phys.* **67**, 599 (1990).
- ¹²R. T. Carline, C. Pickering, D. J. Robbins, W. Y. Leong, A. D. Pitt, and A. G. Cullis, *Appl. Phys. Lett.* **64**, 1114 (1994).
- ¹³C. Pickering, R. T. Carline, D. J. Robbins, W. Y. Leong, S. J. Barnett, A. D. Pitt, and A. G. Cullis, *J. Appl. Phys.* **73**, 239 (1993).
- ¹⁴P. G. Snyder, J. A. Woolam, S. A. Alterovitz, and B. Johs, *J. Appl. Phys.* **68**, 5925 (1990).
- ¹⁵R. Bisaro, J. Magarino, N. Proust, and K. Zellama, *J. Appl. Phys.* **59**, 1167 (1986).
- ¹⁶F. R. L. Schoening, J. Van Niekerk, and R. A. W. Haul, *Proc. Phys. Soc. London, Sect. B* **65**, 528 (1952).
- ¹⁷H. P. Klug and L. E. Alexander, in *X-ray Diffraction Procedures for Polycrystalline and Amorphous Materials* (Wiley, New York, 1954), Chap. 9, p. 491.
- ¹⁸E. L. Mathe', J. G. Maillou, A. Naudon, E. Fogarassy, M. Elliq, and S. De Unamuno, *Appl. Surf. Sci.* **43**, 142 (1989).
- ¹⁹Y. Mishima, M. Takei, T. Uematsu, N. Matsumoto, T. Kakehi, U. Wakino, and M. Okabe, *J. Appl. Phys.* **78**, 217 (1995).
- ²⁰J. Narayan and C. W. White, *Appl. Phys. Lett.* **44**, 35 (1984).
- ²¹Y. Morita and T. Noguchi, *Jpn. J. Appl. Phys., Part 2* **28**, L309 (1989).
- ²²S. M. Sze, *Physics of Semiconductor Devices* (Wiley, New York, 1981).
- ²³D. E. Aspnes, A. A. Studna, and E. Kinsbron, *Phys. Rev. B* **29**, 768 (1984).
- ²⁴S. Bouladakis, S. Logothetidis, and S. Ves, *J. Appl. Phys.* **72**, 3648 (1992).
- ²⁵B. D. Cullity, in *Elements of X-ray Diffraction* (Addison-Wesley, Reading, MA, 1967), Chap. 9, p. 264.
- ²⁶S. Ghosh, A. Dasgupta, and S. Ray, *J. Appl. Phys.* **78**, 3200 (1995).
- ²⁷E. C. Freeman and W. Paul, *Phys. Rev. B* **20**, 716 (1979).
- ²⁸A.-M. Dutron, E. Blanquet, N. Bourhila, R. Madar, and C. Bernard, *Thin Solid Films* **259**, 25 (1995).